



CHAPTER IV

RESULTS AND DISCUSSION

4.1 Catalyst Characterization

This research studied the catalytic activity of CaO–ZnO as a heterogeneous basic catalyst for biodiesel production via transesterification reaction in a batch reactor. In order to investigate the optimum conditions for this reaction, the catalyst was varied with many parameters, such as amount of Ca loading on ZnO support, calcination temperature, and type of catalyst preparation on the biodiesel yield. In order to explain the catalytic activity of the prepared catalysts, the fresh and spent catalysts were characterized by several techniques, such as XRD, FTIR, SEM, TPR, XRF, and titration method.

4.1.1 X-ray Fluorescence Spectroscopy (XRF)

The chemical compositions of the whole samples were summarized in Table 4.1. The synthesized catalysts have the values of metal concentrations closely to those of expected values. Upon the durability testing of the catalysts, as shown in Table 4.2, it was found that the %Ca of the spent catalysts decreased with increasing numbers of running time of reaction, as confirmed by XRD results.

Table 4.1 Chemical compositions of the fresh catalysts by using XRF measurement.

Samples	Calcination temperature (°C)	Element compositions (wt%)		Synthesized Ca/Zn ^a	Expected Ca/Zn
		Ca	Zn		
<i>Co-precipitation</i>					
CaO–ZnO (1:5)	800 (6 h)	13.12	86.88	0.25	0.20
CaO–ZnO (1:3)	800 (6 h)	19.11	80.89	0.39	0.33
CaO–ZnO (1:1)	800 (6 h)	38.53	61.47	1.02	1.00
CaO–ZnO (3:1)	800 (6 h)	72.50	27.50	4.30	3.00
CaO–ZnO (1:3)	600 (6 h)	17.83	82.17	0.35	0.33
CaO–ZnO (1:3)	900 (6 h)	17.06	82.94	0.34	0.33
<i>Incipient wetness impregnation</i>					
CaO–ZnO (1:5)	800 (6 h)	12.82	87.18	0.24	0.20
CaO–ZnO (1:3)	800 (6 h)	26.50	73.50	0.59	0.33
CaO–ZnO (1:1)	800 (6 h)	39.56	60.44	1.07	1.00
CaO–ZnO (3:1)	800 (6 h)	71.55	28.45	4.10	3.00
CaO–ZnO (1:3)	600 (6 h)	22.66	77.34	0.48	0.33
CaO–ZnO (1:3)	900 (6 h)	25.10	74.90	0.55	0.33

^aCalculated from XRF measurement.

Table 4.2 Comparison between the chemical compositions of the fresh and spent catalysts by using XRF measurement.

Samples	Calcination temperature (°C)	Element compositions (wt%)		Synthesized Ca/Zn	Expected Ca/Zn
		Ca	Zn		
<i>Co-precipitation</i>					
CaO–ZnO (1:3) Fresh catalyst	800 (6 h)	19.11	80.89	0.39	0.33
CaO–ZnO (1:3) Spent 1 ^a	800 (6 h)	16.96	83.04	0.33	0.33
CaO–ZnO (1:3) Spent 2 ^b	800 (6 h)	12.89	87.11	0.24	0.33
CaO–ZnO (1:3) Spent 3 ^c	800 (6 h)	12.09	87.91	0.22	0.33
<i>Incipient wetness impregnation</i>					
CaO–ZnO (1:3) Fresh	800 (6 h)	26.50	73.50	0.59	0.33
CaO–ZnO (1:3) Spent 1	800 (6 h)	26.34	73.66	0.58	0.33
CaO–ZnO (1:3) Spent 2	800 (6 h)	23.44	76.56	0.50	0.33
CaO–ZnO (1:3) Spent 3	800 (6 h)	17.40	82.60	0.34	0.33

^a 1st running time of reaction^b 2nd running time of reaction^c 3rd running time of reaction

4.1.2 X-ray Diffraction (XRD)

The XRD patterns of ZnO and CaO–ZnO mixed oxides catalysts with various Ca:Zn atomic ratios for both preparation techniques are shown in Figure 4.1a) (CP) and b) (IWI). The intensities of diffraction peaks at 31.76° , 34.42° , 36.25° , 47.50° , 56.50° , 62.76° , 66.33° , 67.83° , 68.99° , 72.50° , and 76.91° represented the characteristic crystallinity of ZnO substance, which was similar to previous work (Taufiq-Yap *et al.*, 2011). Along with the same trends of Ca–Zn mixed oxides catalysts in both preparation techniques, the intensities of CaO diffraction peaks, detected as 32.37° , 37.62° , 53.99° , 64.37° , and 67.49° (Ngamcharussrivichai *et al.*, 2008), became more pronounced when increasing the Ca concentration. This could be implied that the CaO particles started to be generated as a functional of Ca:Zn atomic ratio. In contrast, the diffraction of ZnO showed the opposite trends in intensities when high Ca was registered, attributing to the new formation of CaO phase in Ca–Zn binary system.

In comparison to the CaO peaks of the catalysts prepared by CP technique, the sharpness peaks were detected from catalyst prepared by IWI technique, indicating that the crystallite structure of CaO particles might be formed as a cluster or larger size in every Ca:Zn atomic ratios via this technique. In the presence of high Ca content, the CaO crystallite size became larger. Interestingly, CaO diffractions of catalyst prepared by CP technique had lower values, which suggested that the IWI technique could give higher crystallinity of CaO than that of CP technique. As mentioned previously, it should be noted that the catalytic activity of CaO–ZnO catalysts strongly depended on the catalyst preparation. This was reasonable to conclude that the IWI technique is more efficient than CP technique in term of structural effect. The crystallite sizes of ZnO and CaO have been calculated by using the Scherrer's equation and summarized in Table 4.3. It is clearly seen that the crystallite sizes of CaO (IWI) increased from 40 nm to 72 nm when increasing the Ca:Zn from 1:5 to 3:1. Nonetheless, the crystallite sizes of ZnO decreased from 51.84 to 46.79 nm when increasing the Ca:Zn from 1:5 to 1:1. These values could possibly confirm the existence of the CaO cluster formation since the overall trends were still consistent with the characteristic peak intensities. Interestingly, this trends did not occur in the catalysts prepared by CP technique; (i) the crystallite sizes of

CaO oppositely decreased (99.34 nm to 53.35 nm) with increasing Ca contents, and (ii) the fluctuation of ZnO crystallite sizes occurred in the range of 37.24–52.18 nm. This could be implied that the variation of Ca loading with CP technique did not promote the growth in CaO crystallite size, when compared with that of IWI technique.

As varying the calcination temperature, as illustrated in Figure 4.2a) (CP) and b) (IWI), the XRD intensities of ZnO and CaO became detectable after rising the calcination temperature up to 900 °C for both preparation techniques, attributing to improvement in crystallinity of CaO and ZnO. According to the increment in peak intensities, the results revealed that two possible mechanisms could be occurred in the highest calcination temperature in ordering; (i) CaO started to separate from the binary mixed oxides system, and (ii) the segregated CaO particles became sintering together to form larger particle sizes. That was reasonable to explain the generating of uninteracted ZnO (high intensities). Thus, the activities of these catalysts could be diminished by the sintering effect. Similar kinds of observation have been reported by Ngamcharussrivichai and coworker (2008). Focusing on the calculated crystallite sizes, both preparation techniques (CP and IWI) represented the increasing of ZnO crystallite sizes with calcination temperature, while those of CaO showed the negative trends in CP (from 89.35 to 52.52 nm) and the unchanged crystallite sizes (~41 nm) in IWI catalysts. Our results suggested that the sintering effect of CaO particle by high thermal treatment could not be confirmed by the crystallite size. Thus, the SEM images must be required to proof the existence of CaO sintering.

Regarding to another phenomenon, the very weak peak of CaCO₃ ($2\theta = 29.56^\circ$) could be detected at the lowest thermal treatment (600 °C) for CP technique, corresponding to the remaining carbonate group depositing on the surface of the catalyst. In the other words, an incompletely changed form of CaCO₃ → CaO could not be efficiently happened when performing at low calcination temperature (Ngamcharussrivichai *et al*, 2008). Consequently, there was no peak of CaO presented in the lowest calcination temperature, so it was difficult to estimate the crystallite size of CaO in this case. However, no peaks of CaCO₃ existed with

applying high treating temperature (>600 °C). Thanks to the decomposition of carbonate modeling in Ca–Zn mixed precipitate at high calcination temperature (800 °C), the CaCO_3 was decomposed to CaO particle and CO_2 gas, and this product gas then diffused out of the pore of the catalyst where the CO_2 film was still surrounding (Ngamcharussrivichai *et al*, 2008). This kind of phenomenon has already been reported over MgCO_3 (El-Shobaky and Mostafa, 2003). That was the reason why the catalytic performance was improved at 800 °C thermal treating. However, the remaining carbonate group was not presented on the surface of catalysts prepared by IWI technique at the lowest calcination temperature, and the CaO diffraction peaks were also detectable, implying that the complete carbonate decomposition has been already provided during the preparation step.

Figure 4.3 illustrates the XRD patterns of both fresh and spent catalysts for comparison purposes. The catalysts were continually tested for 2 cycles: the 1st run and the 2nd run. It was found that the overall spent catalysts showed the disappearance in CaO with the number of testing cycle, indicating that the CaO was leached out from the surface of both CP and IWI catalysts. Taking into account with the diffraction peaks of CaO of the spent IWI catalyst, the CaO phase was still remain on the catalyst's surface after completing two cycles of testing, whereas the CaO leaching out of the spent CP catalyst was more pronounced since the first cycle. Correlating with the rate of CaO leaching, IWI sample exhibited less leaching rate of Ca, compared with that of the spent CP catalyst, which was confirmed in Table 4.5.

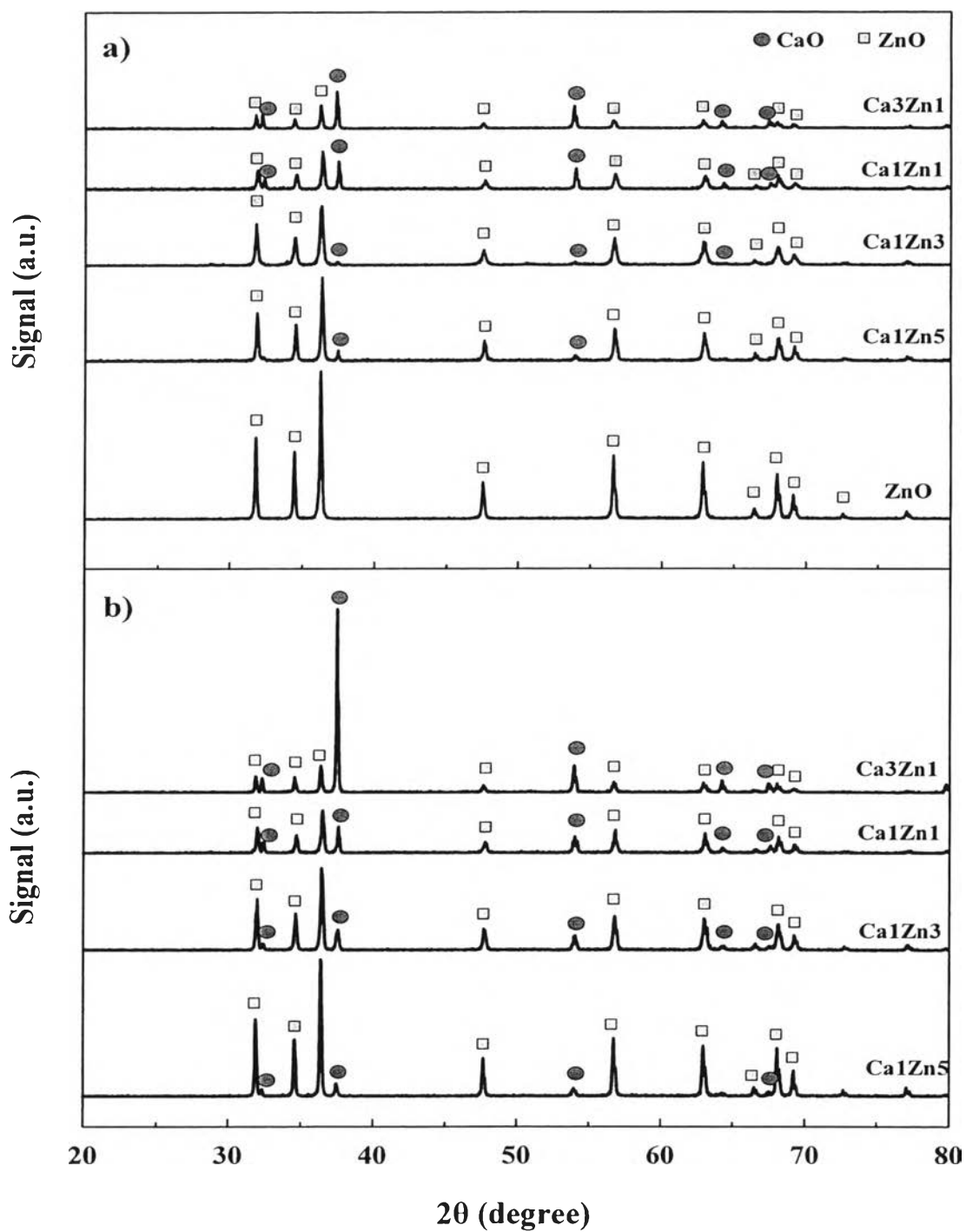


Figure 4.1 XRD patterns of ZnO and Ca–Zn mixed oxides catalysts with various Ca:Zn atomic ratios: a) CP and b) IWI techniques.

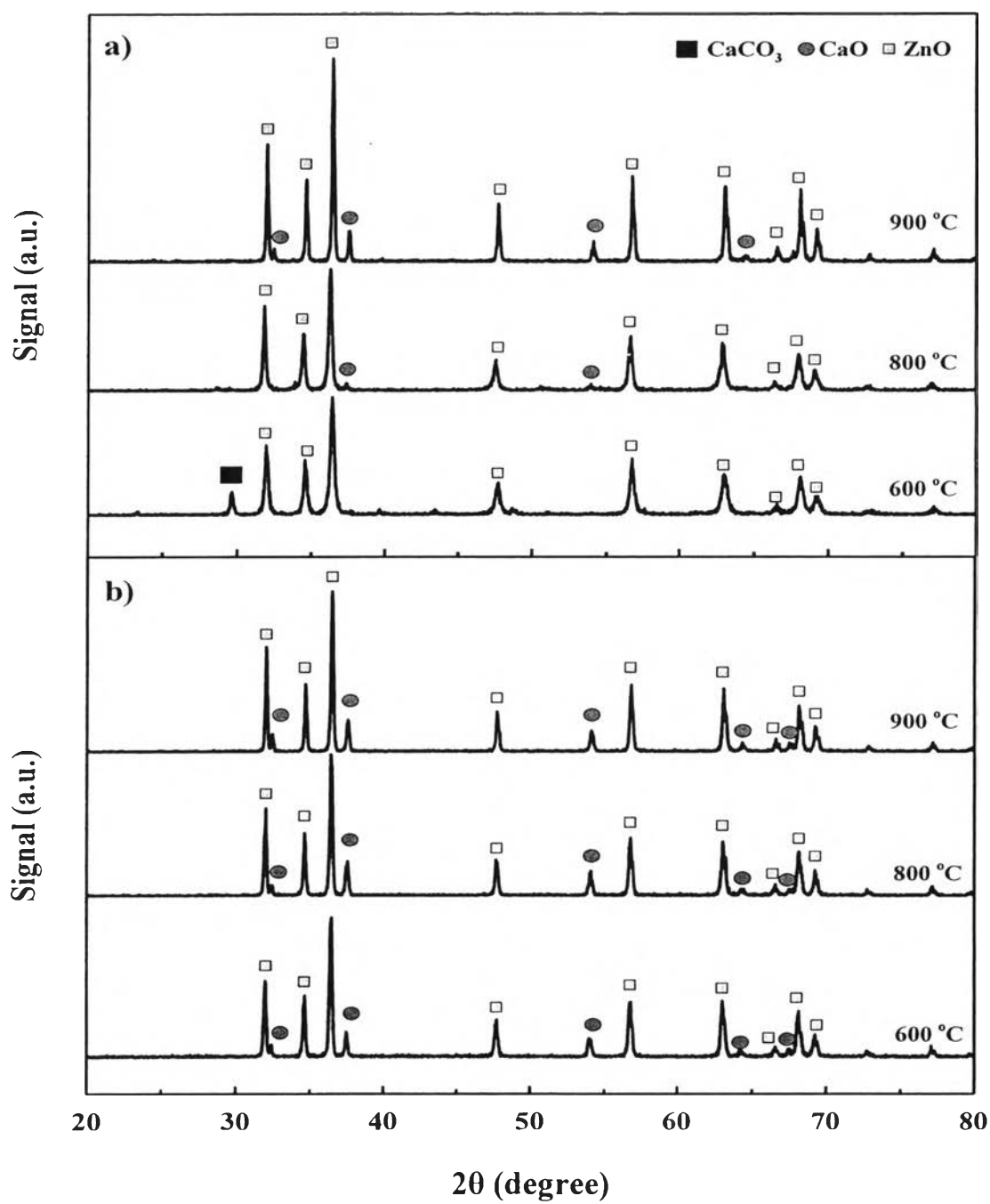


Figure 4.2 XRD patterns of Ca_1Zn_3 catalysts calcined at different temperatures: a) CP and b) IWI techniques.

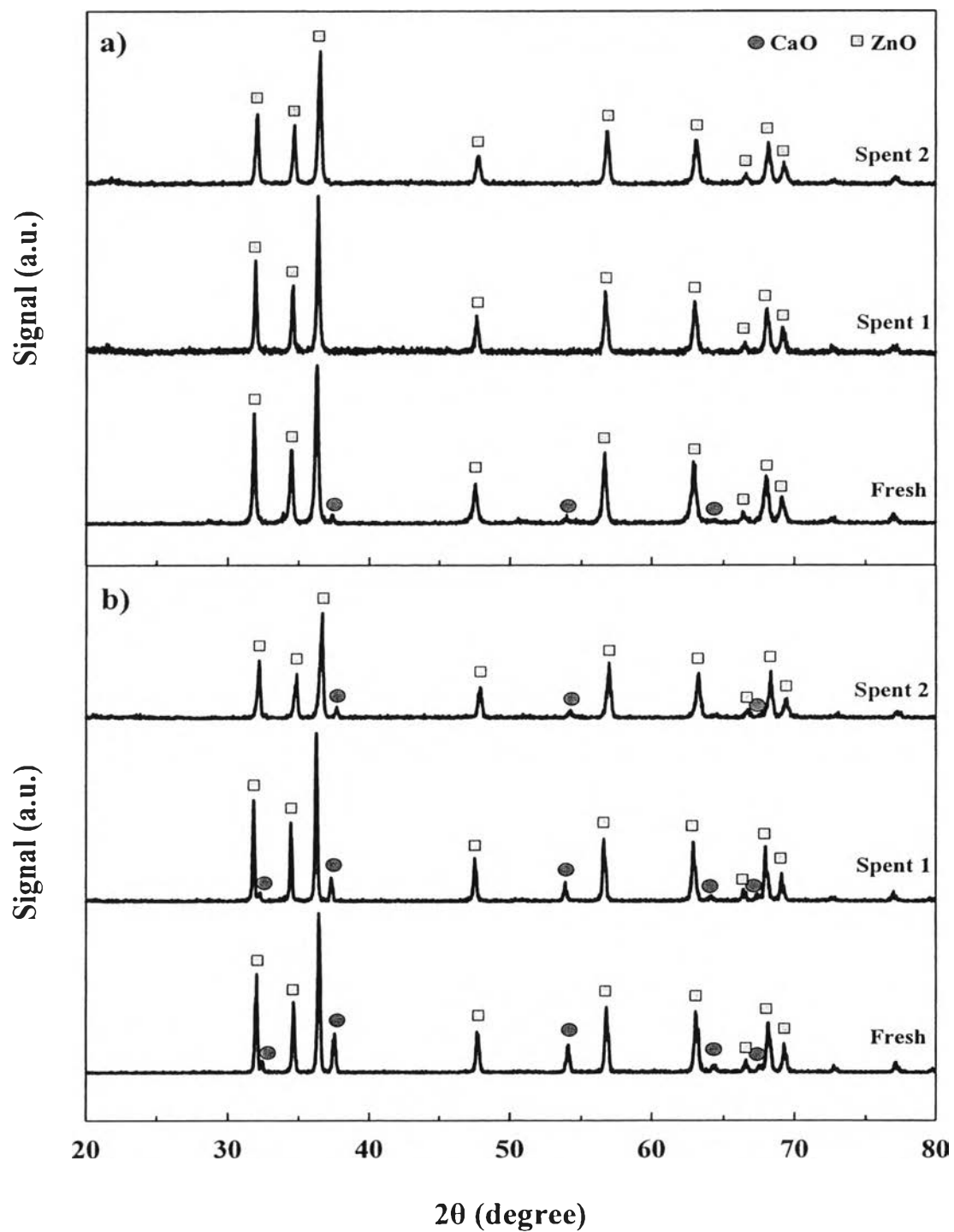


Figure 4.3 XRD patterns of Ca_1Zn_3 catalysts after durability testing: a) CP and b) IWI techniques.

Table 4.3 Chemical-physical properties of the CaO–ZnO fresh catalysts.

Samples	Calcination temperature (°C)	Crystallite size (nm) ^a		CaO–ZnO particle sizes (μm) ^b
		CaO*	ZnO**	
<i>Co-precipitation</i>				
CaO-ZnO (1:5)	800 (6 h)	99.34	48.10	0.33
CaO-ZnO (1:3)	800 (6 h)	89.35	37.24	0.35
CaO-ZnO (1:1)	800 (6 h)	65.73	41.50	0.43
CaO-ZnO (3:1)	800 (6 h)	53.35	52.18	0.53
CaO-ZnO (1:3)	600 (6 h)	-	30.53	0.10
CaO-ZnO (1:3)	900 (6 h)	52.52	50.28	0.42
<i>Incipient wetness impregnation</i>				
CaO-ZnO (1:5)	800 (6 h)	40.36	51.84	0.43
CaO-ZnO (1:3)	800 (6 h)	41.91	47.56	0.48
CaO-ZnO (1:1)	800 (6 h)	43.12	46.79	0.48
CaO-ZnO (3:1)	800 (6 h)	72.09	56.52	0.48
CaO-ZnO (1:3)	600 (6 h)	41.95	42.84	0.24
CaO-ZnO (1:3)	900 (6 h)	41.54	51.22	0.58

^aCalculated from the Scherrer's equation.

*Averaged from the diffractions of 32.37°, 37.62°, and 53.99°.

**Averaged from the diffractions of 31.76°, 34.42°, and 36.25°.

^bEstimated from SEM images.

Table 4.4 Mean crystallite sizes of the spent CaO–ZnO catalysts.

Samples	Calcination temperature (°C)	Crystallite size (nm)	
		CaO	ZnO
<i>Co-precipitation</i>			
CaO-ZnO (1:3) Fresh catalyst	800 (6 h)	89.35	37.24
CaO-ZnO (1:3) Spent 1	800 (6 h)	-	43.62
CaO-ZnO (1:3) Spent 2	800 (6 h)	-	36.91
<i>Incipient wetness impregnation</i>			
CaO-ZnO (1:3) Fresh catalyst	800 (6 h)	41.91	47.56
CaO-ZnO (1:3) Spent 1	800 (6 h)	58.29	54.56
CaO-ZnO (1:3) Spent 2	800 (6 h)	54.12	34.40

4.1.3 Temperature-Programmed Reduction (TPR)

The TPR profiles of CaO–ZnO catalysts with various Ca:Zn atomic ratios were recorded in Figure 4.4a) (CP) and b) (IWI). Three broadened reduction peaks of ZnO were observed at 351, 458, and 637 °C. When adding Ca to form the Ca–Zn binary system for both CP and IWI techniques, the improvement in reducibility was observed noticing from the shifting peaks toward lower temperatures, compared to pure ZnO. The initial activity was then recovered when compared with the pure support.

Focusing on the Ca–Zn mixed oxides catalyst prepared by CP technique, the decrease in hydrogen consumption (relating with the area under peak of ZnO) in the Ca:Zn ratio of 1:5 was observed since some parts of Zn might be incorporated with Ca to form Ca–Zn binary system. Then, the remaining ZnO sites (after being reduced) were lower than those of pure ZnO support. After increasing the Ca:Zn ratio to 1:3, the shifting reduction peak to lower temperature (600 °C)—representing the change in interaction and upgrading of CaO–ZnO reducibility—was observed, while the hydrogen consumption became much higher. This could be implied that some of CaO registration could possibly help promote the ZnO reduction sites during the preparation step. Nevertheless, in the presence of high Ca loading (Ca:Zn = 1:1 and 3:1), the slight shifting in peaks toward higher temperature were discovered (608 and 619 °C), indicating that the separation of ZnO from Ca–Zn binary system became favored. On the other hand, the strength of Ca–Zn interaction could be disturbed when registering an excess Ca concentration (Ca:Zn>1:3). Interestingly, the lowest hydrogen consumption was observed for the high Ca contents (Ca:Zn = 1:1 and 3:1), indicating that the agglomeration or sintering of CaO particles might inhibit or block the surface area of reduction sites, then the number of hydrogen adsorbed was low. As mentioned previously, the Ca–Zn interaction at the suitable Ca:Zn ratio of 1:3 could play an important role for enhancing the catalytic activity. Likewise, the lowest catalytic performance of CaO–ZnO catalysts was found in very high Ca:Zn ratio of 4 since the CaO became separating to form the film coating on the ZnO surface, which could be evidenced by SEM technique (Ngamcharussrivichai *et al*, 2008).

In the case of IWI catalysts, the shifting reduction peaks toward lower temperature appeared for all Ca loadings, compared to pure ZnO. This kind of behavior also confirmed the combination of homogeneous Ca–Zn interaction, resulting in increasing the reducibility of ZnO (reduced much easier). Interestingly, no significant differences among the reduction peaks of high Ca:Zn ratios (1:3–3:1) were observed, even the width of the reduction peaks. In some cases, it has been proposed that the width of the reduction peak could relate the dispersion of metal briefly (Biswas and Kunzru, 2007). In our results, we interpreted that there was no change in dispersion of CaO particles in the presence of high Ca contents. Linking with the catalytic activity, the unchanged dispersion of CaO could be the main factor which exhibited similarity in 80% biodiesel yield in the Ca:Zn range of 1:3–3:1. In addition, the hydrogen consumption in all reduction peaks of high Ca loading (Ca:Zn = 1:3, 1:1, and 3:1) were also the same. This could be related with the unchanged in CaO particle sizes during the Ca variation. Consequently, the similarity activity could be provided with the unchanged particle size. We suggested that the size of CaO particle might be one of the main factors to control the catalytic activity.

In order to compare two types of preparation techniques, it was strongly defined the criteria of chemical properties that the catalytic activity depends on the metal–metal interaction, reducibility, particle size, and dispersion. It should be noted that the beneficial structural effect in IWI preparation was; (i) the stable dispersion and particle size, which could be concluded that the addition of Ca could stabilize its particle size, and (ii) the CaO sintering could be avoided or prevented by loading Ca with IWI technique. For the advantage of CP preparation technique, the better dispersion and the easiest reducibility could be provided with the suitable or optimal Ca registration, but the CaO particle size was less stable than that of CP. In the realistic application, our recommendation in catalyst preparation option was “depend on what” since both techniques have the pros and cons in technical terms.

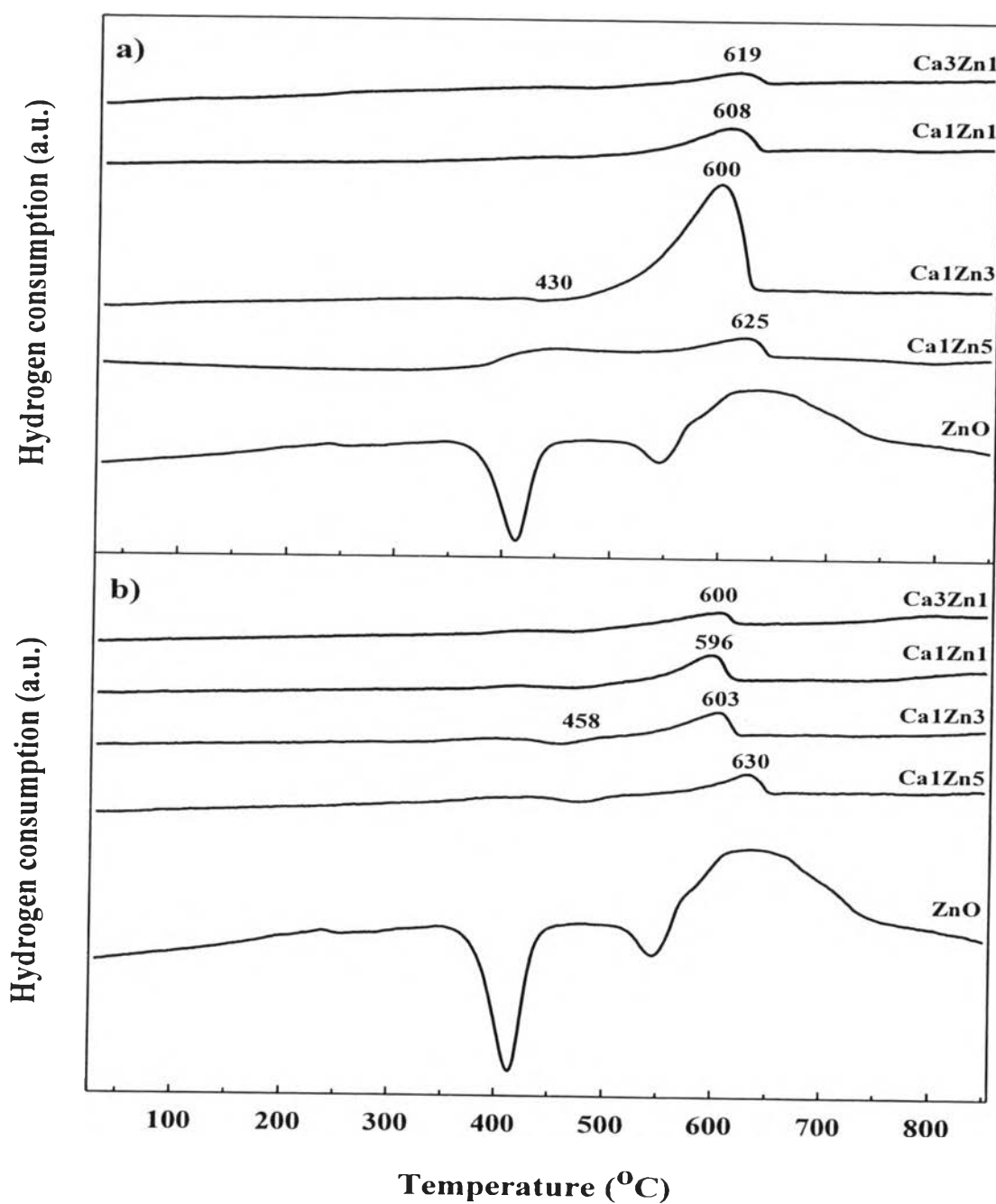


Figure 4.4 TPR profiles of ZnO and Ca-Zn mixed oxides with various Ca:Zn atomic ratios: a) CP and b) IWI techniques.

From Figure 4.5, the effect of calcination temperature on the catalytic activity was also tested for the catalysts prepared by CP (a) and IWI (b) techniques. For CP catalysts calcined at 600 °C, the reduction of mixed CaO–ZnO peak shifted toward higher temperature (close to ZnO region), compared to 800 °C. To explain this phenomenon using XRD technique, this low temperature might be not suitable for the creation of CaO–ZnO mixed phase due to the fact that the CaCO₃ could not decompose to CaO at this low temperature, so the probability of CaO formation, including interaction, might be not favored. As mentioned above, the difficult in mixing ZnO with CaO could happen. That was reasonable for the high area or hydrogen consumption in ZnO without containing CaO. At the highest thermal treatment (900 °C), the trend of shifting peak was similar to that of 600 °C. Moreover, the area of hydrogen consumed was the lowest since the CaO would undergo sintering at this condition (Biswas and Kunzru, 2007). Similar to the previous explanation of Ca:Zn variation, the shift of reduction peak from T_{\max} of 600 °C could be referred to the segregation of some CaO from the region of mixed oxides system to agglomerate with another CaO particle. This CaO segregation behavior also affected in ZnO crystallinity, which was successfully in line with the very high ZnO diffraction peaks—representing the uninteracted ZnO from binary system—, as confirmed by XRD. Finally, the catalytic activity was well-inhibited by the effect of inhomogeneous CaO–ZnO phase in the highest calcination temperature. In addition, the improvement in CaO diffraction peak can be also used as an indicator for proving the CaO sintering.

In the case of IWI samples (Figure 4.5(b)), the results agree well with the XRD results that the sintering of CaO particles was more pronounced with increasing calcination temperature according to the minute amount of hydrogen consumption in the mixed CaO–ZnO reduction peak. Taking into account of the sintering effect, the lacking of significant chemical properties could be related with this phenomenon. Besides, there were the shifts in T_{\max} reduction temperatures of the samples calcined at 600 °C and 900 °C, representing the change in mixed oxides interaction in the CaO–ZnO catalysts during varying the calcination temperature. This could be another main factor for providing inhomogeneous mixed oxides catalyst. Nevertheless, the reason why the T_{\max} shifted to higher or lower reduction

temperature after treating with unsuitable calcination temperatures (600 °C and 900 °C) for the catalysts prepared by both techniques was still unclear.

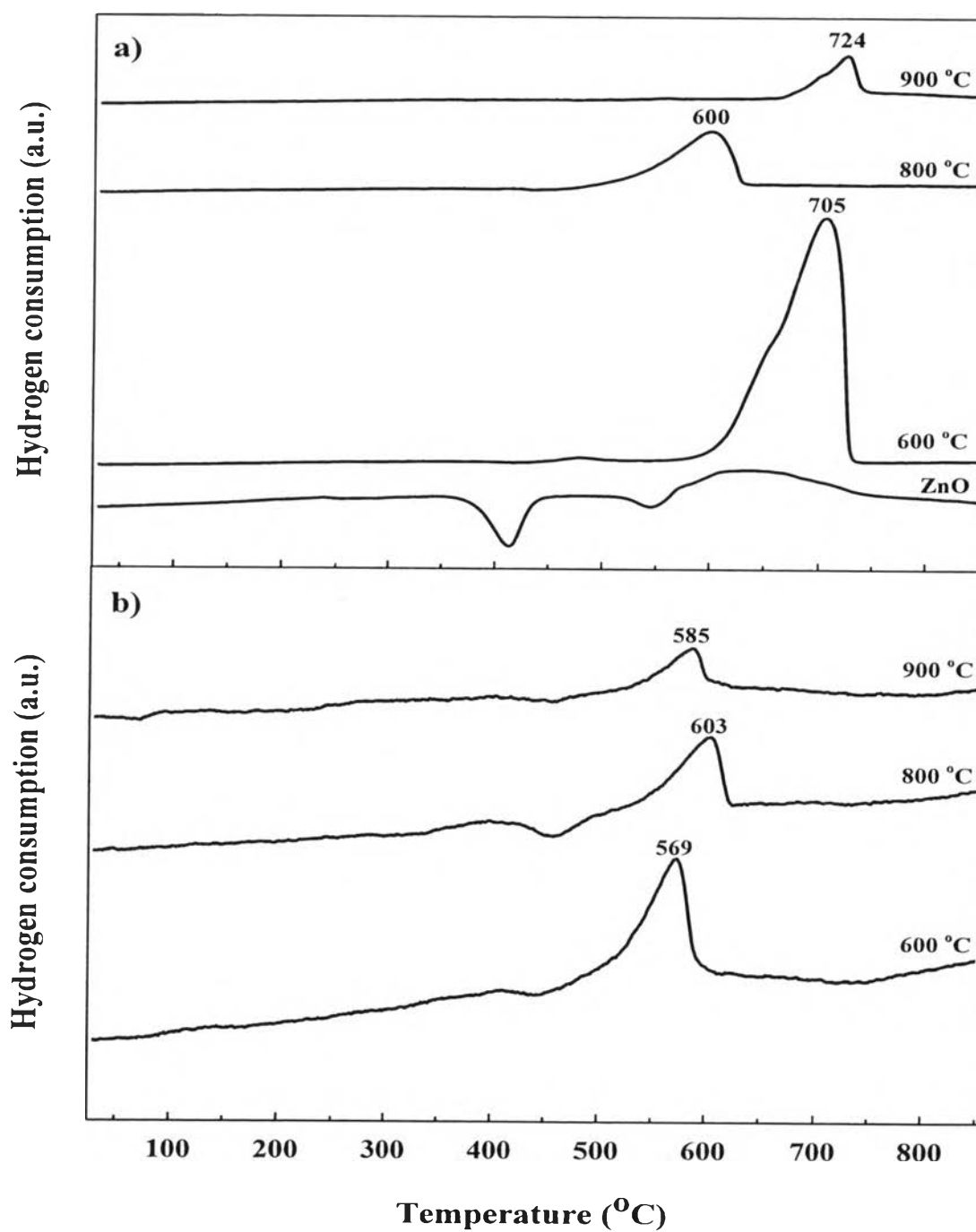
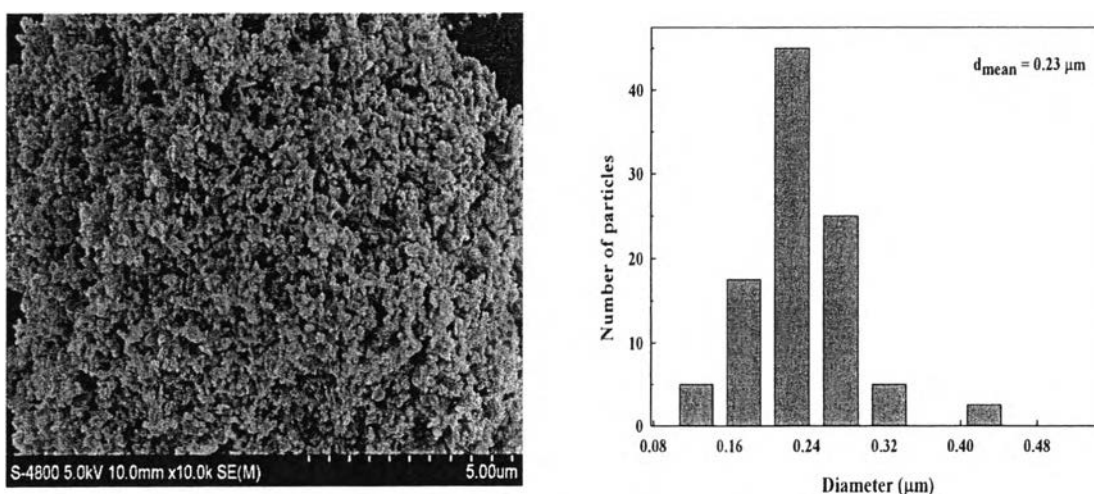


Figure 4.5 TPR profiles of Ca₁Zn₃ catalysts with different calcination temperatures: a) CP and b) IWI techniques.

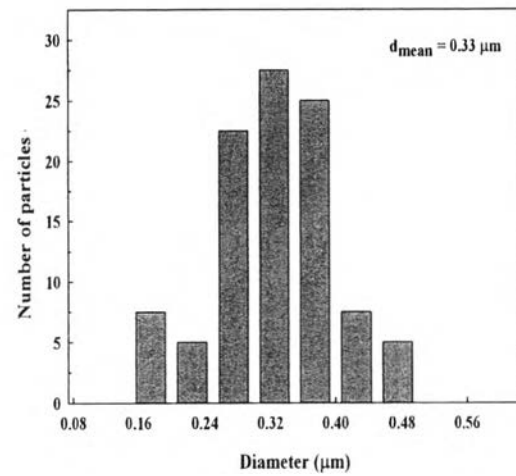
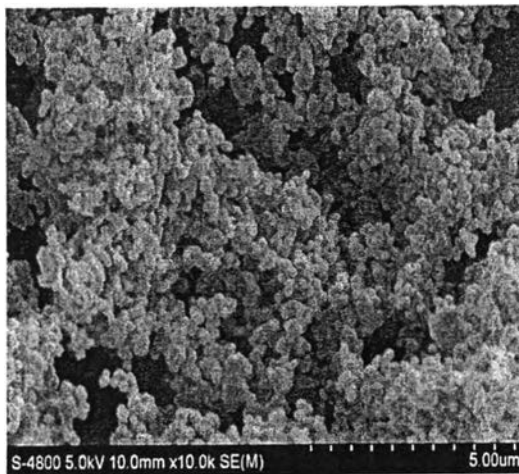
4.1.4 Scanning Electron Microscope (SEM)

According to the morphology and particle size of the catalysts, as imaged in Figure 4.6, it was found in the mixed oxides catalysts that the particle size of the catalyst increased with increasing the percentage of Ca loading for CP catalysts, while the IWI catalysts seemed to stabilize the size of particle (0.43–0.48 μm) in every Ca:Zn atomic ratios. Moreover, the overall structural shape of IWI samples was similar, even at low Ca loading. As mentioned in the previous section, the sintering of CaO particles in CP catalysts could also be confirmed in the catalysts with high Ca:Zn atomic ratio (1:1 and 3:1). The consideration was based on the morphology changed from the very fine CaO particles (0.33 μm) at low Ca loadings to the agglomerated CaO cluster (0.53 μm) at high Ca loadings. It was reasonable to support the highly distributed Ca species upon the surface as a cause of larger particle size.

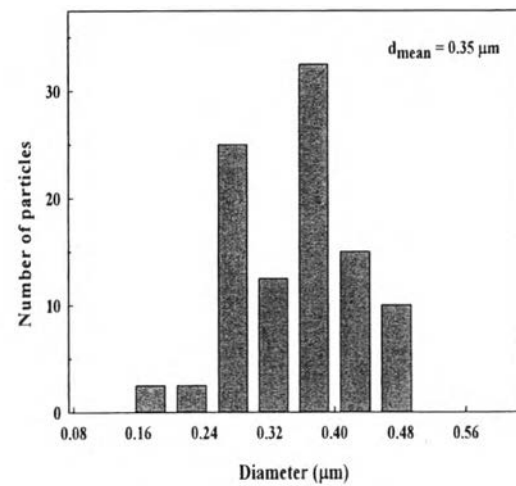
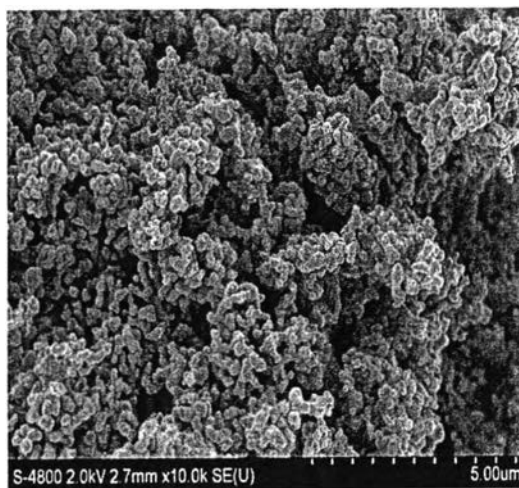
In the part of discussion, the catalytic activity of CP catalysts could be inhibited by the CaO sintering effect— $d_{\text{mean}} > 0.35 \mu\text{m}$ (optimum size)—, whereas the stable sizes for IWI catalysts might be initially approached in the optimal value of 0.48 μm for Ca:Zn > 1:5. Consequently, the optimum and stable sizes for IWI could result in efficient and similar activities.



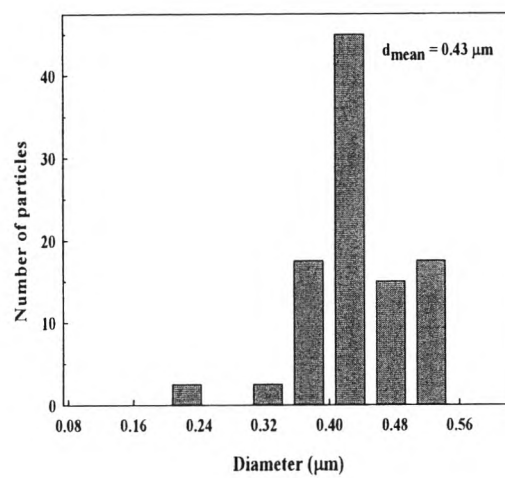
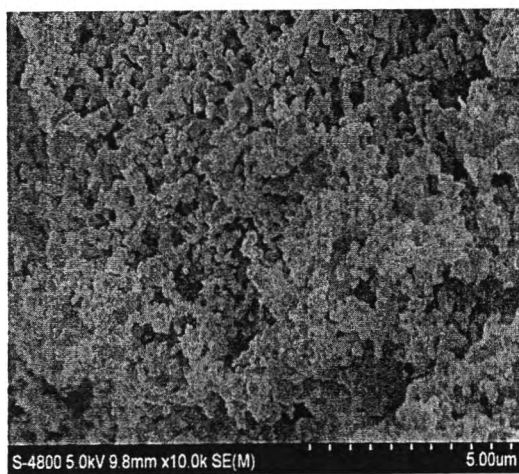
ZnO catalyst



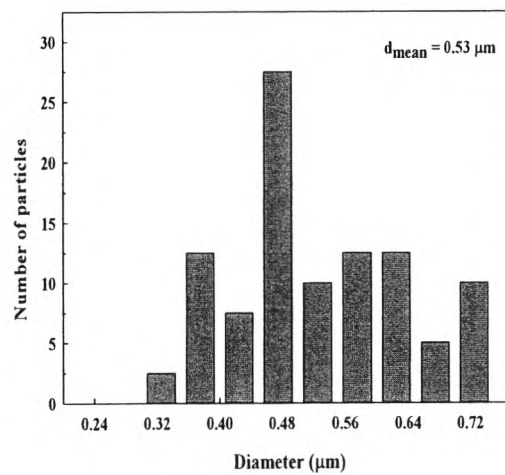
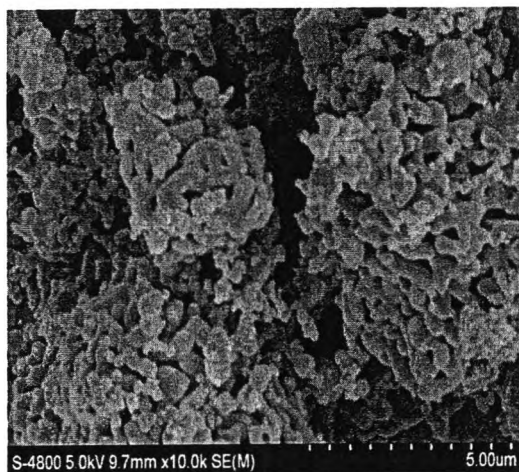
CaO-ZnO (1:5, CP) catalyst



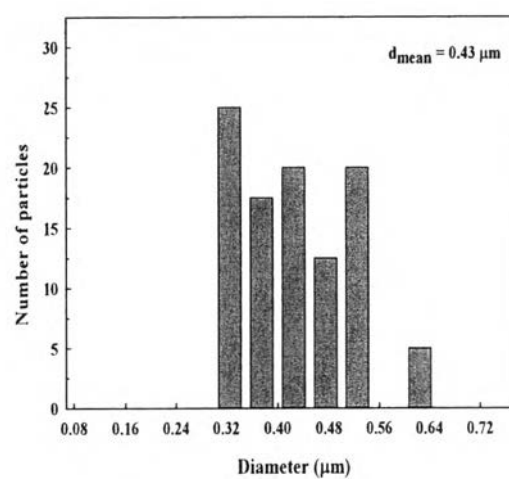
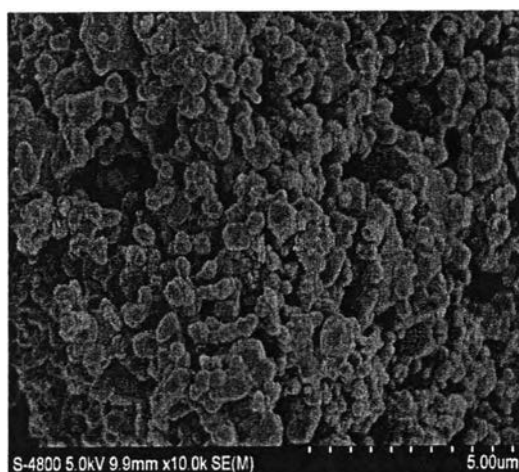
CaO-ZnO (1:3, CP) catalyst



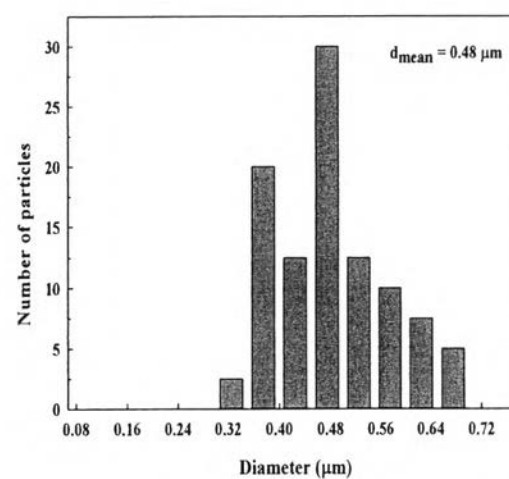
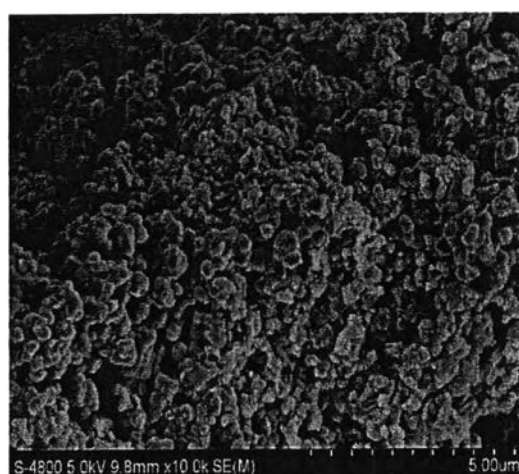
CaO-ZnO (1:1, CP) catalyst



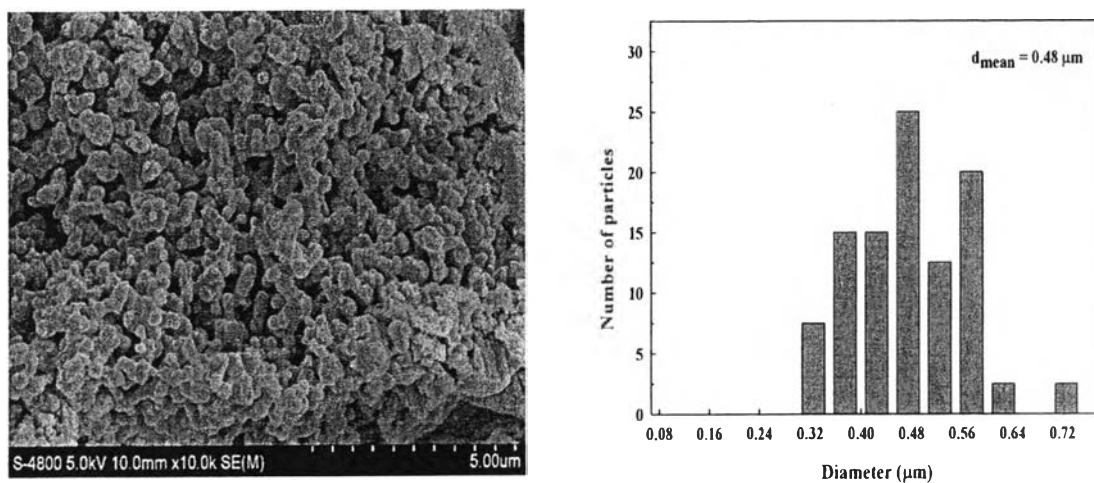
CaO-ZnO (3:1, CP) catalyst



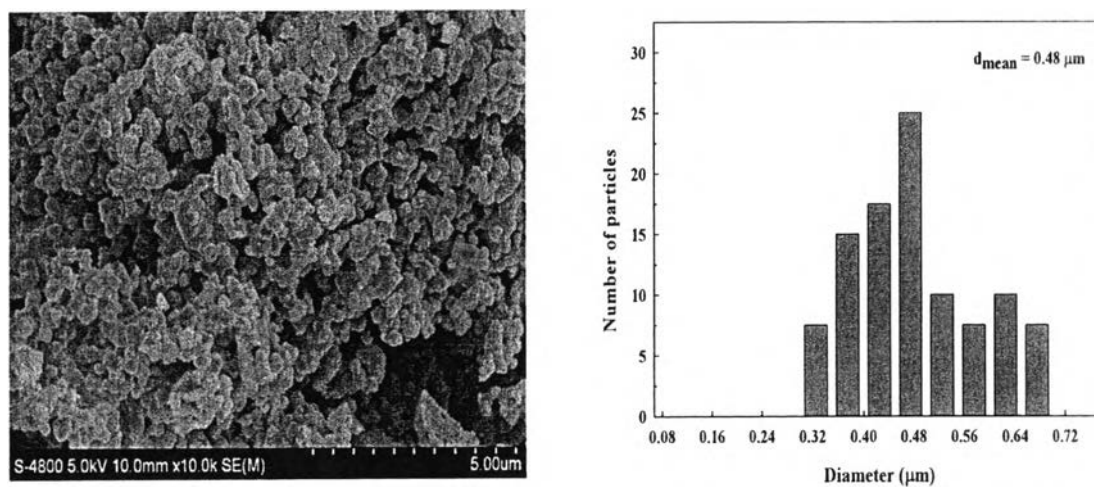
CaO-ZnO (1:5, IWI) catalyst



CaO-ZnO (1:3, IWI) catalyst



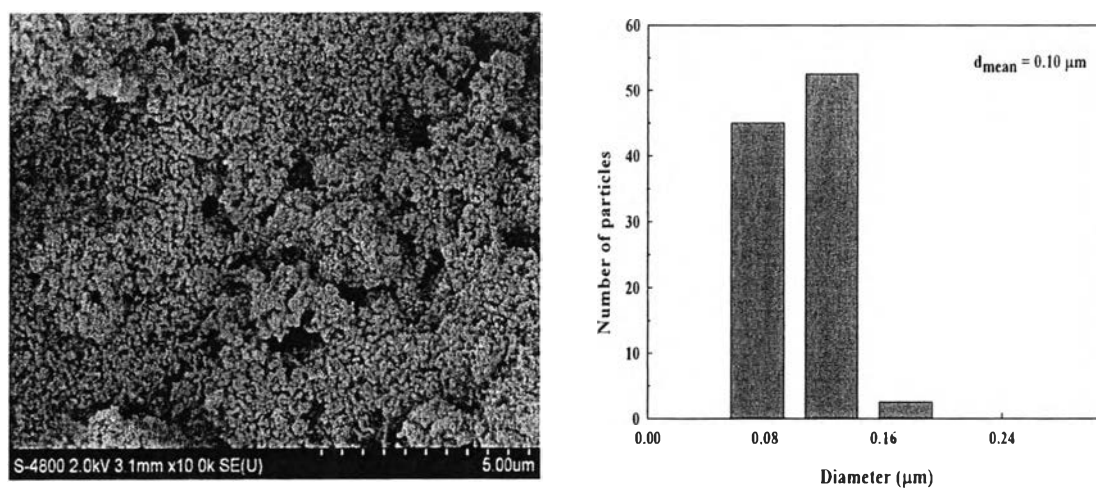
CaO-ZnO (1:1, IWI) catalyst



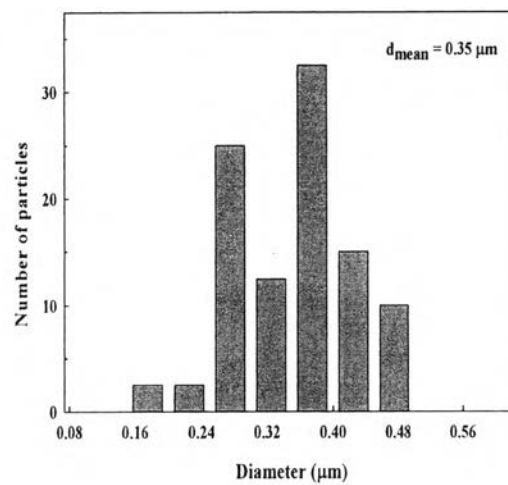
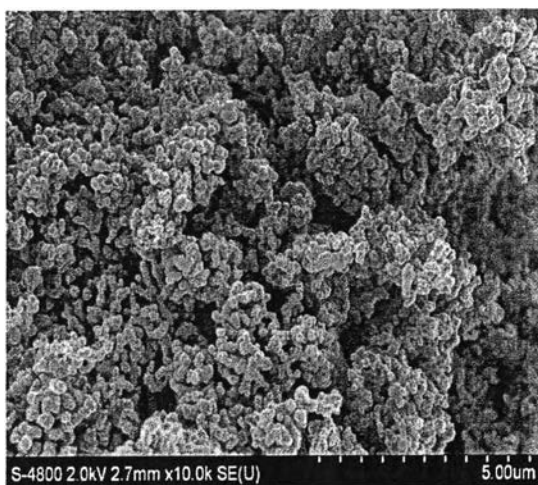
CaO-ZnO (3:1, IWI) catalyst

Figure 4.6 SEM images of ZnO and Ca-Zn mixed oxides catalysts with various Ca:Zn atomic ratios.

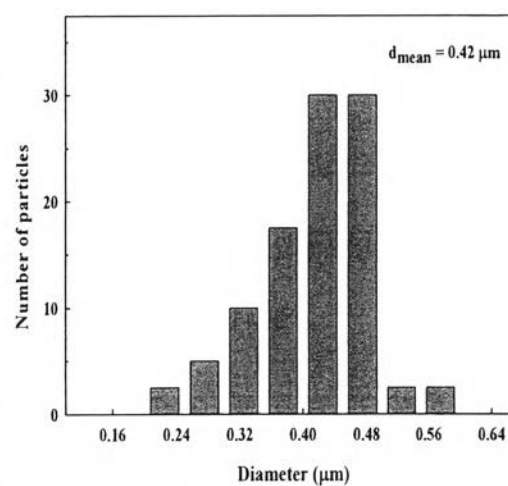
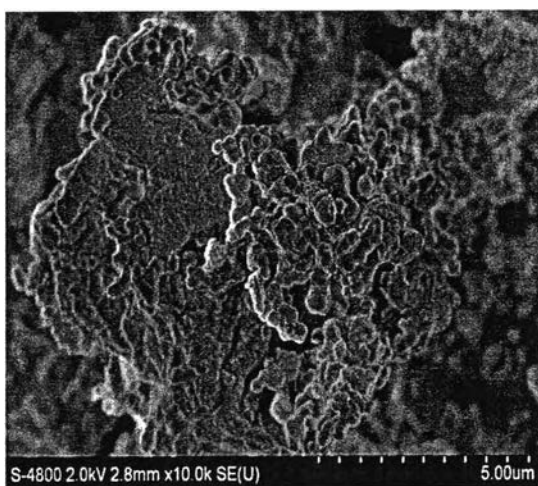
When varying calcination temperature of the CaO–ZnO (Ca:Zn = 1:3) catalysts, the SEM images (Figure 4.7) revealed that the size of CaO cluster was increased with increasing calcination temperature. However, the positive result of upgrading calcination temperature was to provide the optimum size of CaO particle in the catalyst, which might be suitable for the reaction. In terms of electronic effect, Ngamcharussrivichai and coworker (2008) also proposed that the calcination temperature of 600 °C, which is required for the decomposition of CaCO₃ to form CaO, the lower the energy that is consumed in the preparation of active catalyst. For the negative structural change, the highest calcination temperature of 900°C definitely represented the agglomeration of CaO cluster, which could block the active site of the catalyst, so the catalyst was finally deactivated. It can be concluded that the suitable thermal treatment for preparing the active CaO–ZnO catalyst belonged to 800 °C.



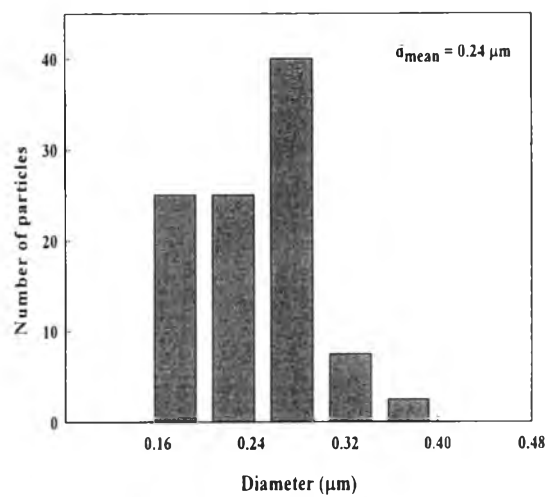
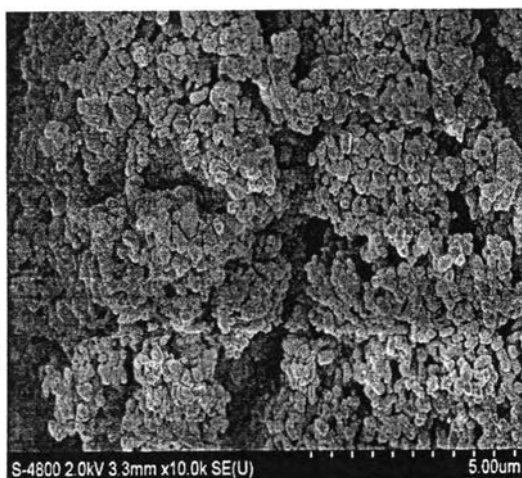
CaO–ZnO (1:3, CP, calcined at 600 °C) catalyst



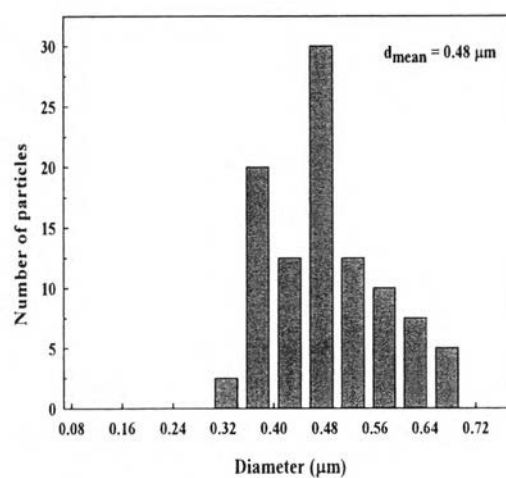
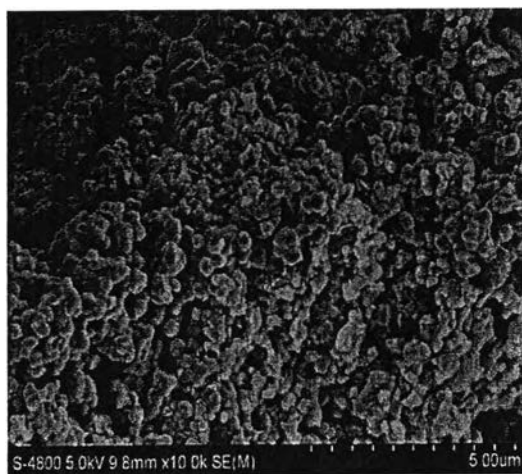
CaO-ZnO (1:3, CP, calcined at 800 °C) catalyst



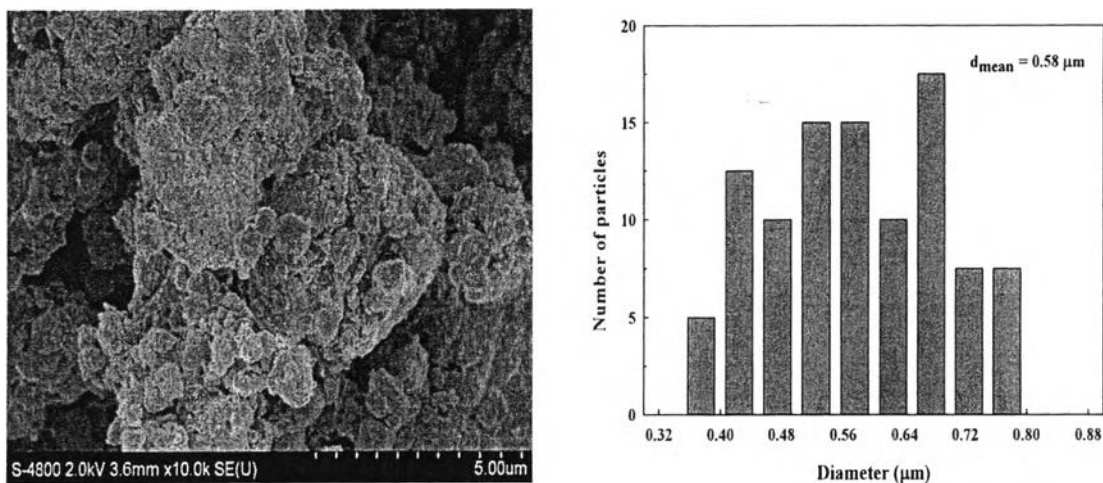
CaO-ZnO (1:3, CP, calcined at 900 °C) catalyst



CaO-ZnO (1:3, IWI, calcined at 600 °C) catalyst



CaO-ZnO (1:3, IWI, calcined at 800 °C) catalyst



CaO–ZnO (1:3, IWI, calcined at 900 °C) catalyst

Figure 4.7 SEM images of CaO–ZnO (Ca:Zn = 1:3) catalysts with various calcination temperatures.

4.1.5 Hammett Indicator

The basic strength, basicity, and Ca leaching of the fresh and spent CaO–ZnO catalysts were recorded in Table 4.5. The basic strength of the catalysts (H_-) was determined by using the following Hammett indicators: bromothymol Blue ($H_- = 7.2$), phenolphthalein ($H_- = 9.8$), Tropaeolin ($H_- = 11$), 2,4-dinitroaniline ($H_- = 15$), and 4-nitroaniline ($H_- = 18.4$). Indeed, all of the fresh catalysts in both preparation techniques achieved high basic strength in the range of 11.0–15.0. In term of basicity measurement, with acid titration technique, the basicity of all fresh samples directly increased with increasing amounts of Ca concentration. Especially, the basicity of catalysts prepared by IWI technique exhibited higher values than those of CP technique in every Ca:Zn ratios. It can be one of the possible factors why the IWI catalysts exhibited much higher activity, when compared with CP catalysts in the same Ca:Zn ratio. However, the catalytic activity of each preparation technique did not follow the trends of basicity when increasing the Ca loading. This could be implied that there must be other factors (not only basicity) which can boost up or slow down the catalyst's ability. Thus, the conclusion based on only basicity was not efficient for evaluating the best catalyst. The authors suggested that the best

catalytic activity might depend on the suitable basicity, structural effect, and electronic effect.

For the basic strength and basicity of the spent catalyst, the results showed that the basic strength and basicity of the fresh catalysts were much higher than those of the spent^{1st} and spent^{2nd} catalysts, indicating that the lacking of basic strength and basicity of the catalysts during the reaction mainly came from the leaching (or dissolved) of Ca substance into the product mixture, the loss in catalytic activity (or low biodiesel yield) was then followed. As evidenced by XRF, a decrease in %Ca of retested catalysts definitely confirmed this leaching phenomenon.

Table 4.5 Summarization of basic strength, basicity, and Ca leaching of the fresh and spent catalysts.

Catalysts	Basic strength (H_-)	Basicity (mmol/g)	Ca leaching (%)
<i>Fresh catalysts</i>			
<i>Co-precipitation</i>			
CaO–ZnO (1:5)	$11.0 < H_- < 15.0$	3.1191	-
CaO–ZnO (1:3)	$11.0 < H_- < 15.0$	4.4826	-
CaO–ZnO (1:1)	$11.0 < H_- < 15.0$	12.4935	-
CaO–ZnO (3:1)	$11.0 < H_- < 15.0$	18.2758	-
<i>Incipient wetness impregnation</i>			
CaO–ZnO (1:5)	$11.0 < H_- < 15.0$	4.5431	-
CaO–ZnO (1:3)	$11.0 < H_- < 15.0$	7.6874	-
CaO–ZnO (1:1)	$11.0 < H_- < 15.0$	15.0100	-
CaO–ZnO (3:1)	$11.0 < H_- < 15.0$	23.5828	-
<i>Spent catalysts</i>			
<i>Co-precipitation</i>			
CaO–ZnO (1:3) (CP) (1)	$7.2 < H_- < 9.8$	0.3407	11.2507
CaO–ZnO (1:3) (CP) (2)	$H_- < 7.2$	0	32.5484
<i>Incipient wetness impregnation</i>			
CaO–ZnO (1:3) (IWI) (1)	$11.0 < H_- < 15.0$	2.2711	0.6038
CaO–ZnO (1:3) (IWI) (2)	$11.0 < H_- < 15.0$	0	11.5472

^aCalculated from XRF measurement

4.1.6 Fourier Transform Infrared Spectrophotometer (FT-IR)

The absorbances of fresh and spent catalysts after durability test were scanned from 3500 cm^{-1} to 1000 cm^{-1} , as shown in Figure 4.8. In comparison to the fresh catalysts (CP and IWI), all spent catalysts obviously showed several characteristic functional groups of oil, such as C-H stretching ($2924\text{--}2850\text{ cm}^{-1}$), C=O stretching (1744 cm^{-1}), C-H bending ($1654\text{--}1368\text{ cm}^{-1}$), and C=C stretching (3014 cm^{-1}), which represented the contamination of biodiesel upon the catalyst's surface. Furthermore, these functional groups also tended to increase with running time, which could be referred to the accumulation of the amounts of biodiesel on the catalyst's surface.

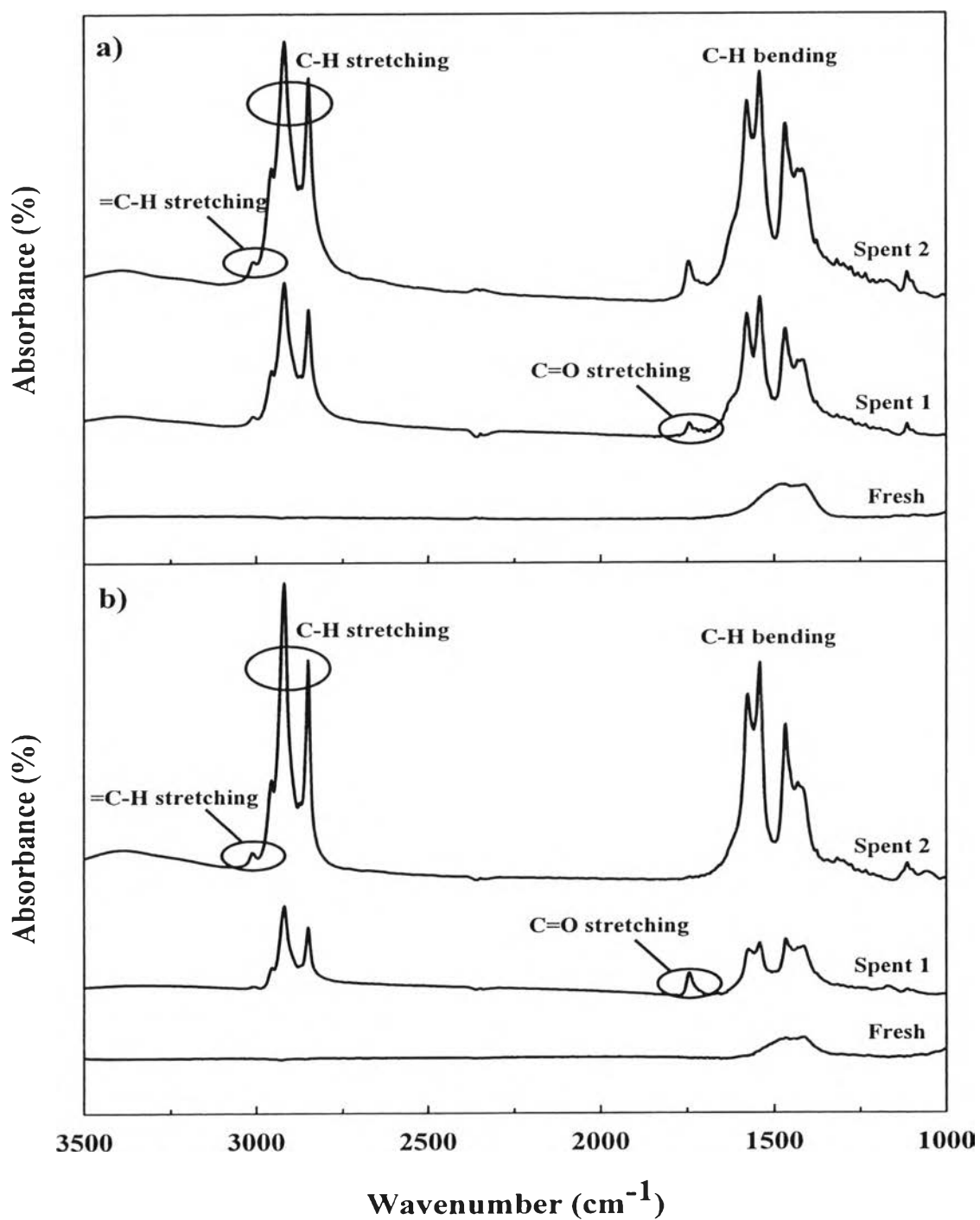


Figure 4.8 FTIR spectra of the spent Ca_1Zn_3 catalysts after durability testing: a) CP and b) IWI techniques.

4.2 Transesterification Reaction

CaO–ZnO was used as a heterogeneous basic catalyst in transesterification reaction. To investigate the optimum conditions of these catalysts in transesterification of palm oil, the starting conditions of transesterification reaction using CaO–ZnO catalyst were 60 °C of the reaction temperature, 300 rpm of stirrer speed, 1:3 atomic ratio of Ca:Zn, 15:1 molar ratio of methanol to oil, and amount of catalyst 6 wt% (based on weight of vegetable oil).

4.2.1 Effect of Reaction Time

The effect of reaction time on the yield of biodiesel, illustrated in Figure 4.9, was tested by using the CaO–ZnO (atomic ratio Ca:Zn = 1:3) catalyst under the conditions of reaction temperature of 60 °C, 300 rpm of stirrer speed, 15:1 molar ratio of methanol to oil, and amount of catalyst 6 wt%. It is well known that the transesterification of palm oil strongly depends on the reaction time (Xie *et al.*, 2007). As varying the reaction time range of 0–12 h, the biodiesel yield seemed to increase proportionally with the reaction time for both preparation techniques (CP and IWI). However, the yield became steadily—nearly equilibrium conversion—when the reaction time was higher than 8 h. According to the initial reaction time (<8 h), the large difference between the sample prepared by CP and IWI was observed. Interestingly, CP catalyst exhibited the rate of reaction faster than that of IWI catalyst, while the reaction rate of IWI sample was favorable at higher reaction time than 8 h. To summarize, the reaction time of 8 h was suggested for being the suitable condition since the reaction time was not too high and also gave the 80% yield of biodiesel production for both preparation techniques.

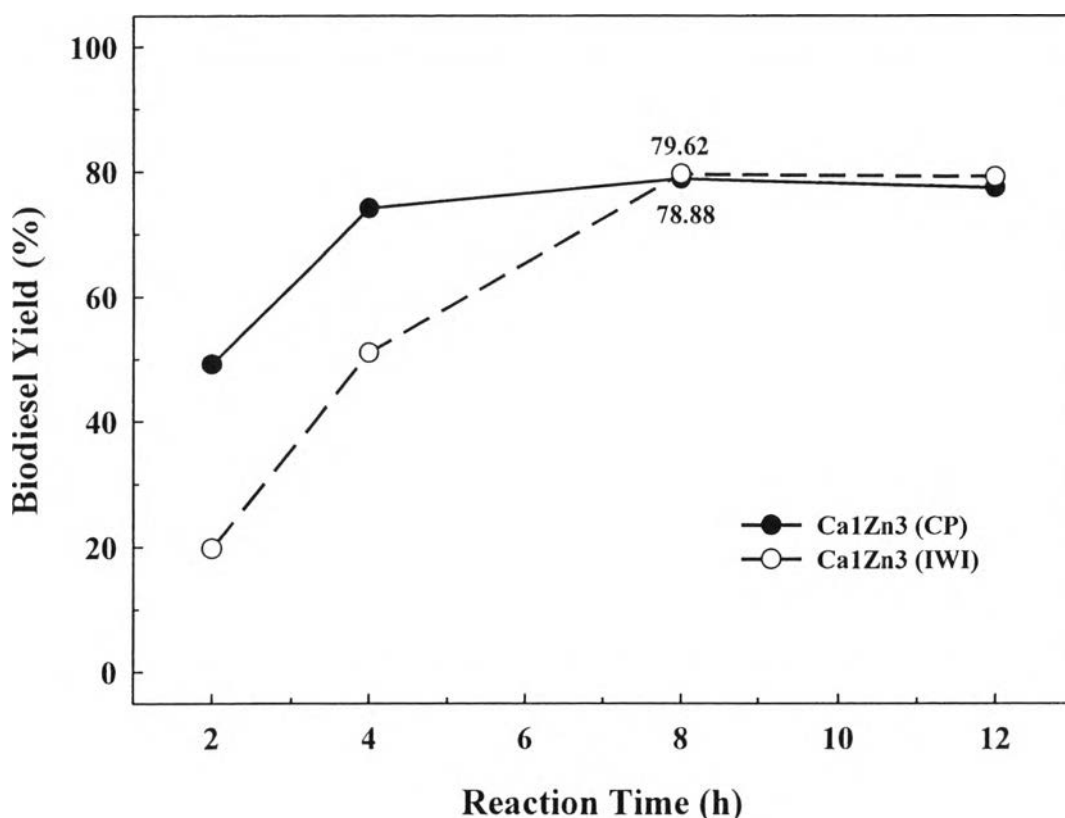


Figure 4.9 Effect of reaction time on biodiesel yield. Reaction conditions: 60 °C of reaction temperature, 1:3 atomic ratio of Ca:Zn, 15:1 molar ratio of methanol to oil, amount of catalyst 6 wt%, and 300 rpm of stirrer speed.

4.2.2 Effect of Calcination Temperature

The effect of calcination temperature (600–900°C) was investigated on the reaction time of 8 h, while the remaining parameters were constantly fixed. Figure 4.10 indicates that both activities of CP and IWI catalysts were improved when calcination temperature was upgraded from 600 °C to 800 °C. However, the highest calcination temperature of 900 °C gave the lowest catalytic activities for both catalysts. Ngamcharussrivichai and coworker (2008) achieved the same trends and proposed that increasing calcination temperature up to 900 °C could significantly decrease the methyl ester content since the sintering of CaO particles could be possibly affected, as evidenced by XRD technique. Furthermore, Boynton (1999) also reported a hard burn effect in the limestone (CaO)—a dense and inactive

substance—where the high calcination temperature could be related with. However, our results suggested that the incomplete decomposition of carbonate species (CO_3^{2-}) at the low calcination temperature of 600 °C might be the main factor for lowering the catalytic activity, which could be confirmed by XRD pattern of CP sample. Even though, there was no carbonate detected in IWI sample, the authors would like to note that the suitable calcination temperature of 800 °C might perform the suitable Ca–Zn interaction in the binary system, when compared to other calcination temperatures (600 °C and 900 °C). The evidence of this type of interaction could be attributed to the shift of T_{max} from 600 °C. However, the reasons why the shift of T_{max} less or higher than 600 °C when increasing or decreasing the calcination temperature from 800 °C, were still unclear. Furthermore, the sintering effect of CaO particles should be one of the importance factor for deactivating the CaO–ZnO catalyst at the highest calcination temperature, as evidences from many previous characterization techniques (TPR, XRD, and SEM). According to the results, the thermal treatment condition of 800 °C should be suitable for the catalyst preparation's condition since it could provide the highest biodiesel (~80%), which was efficient enough for this reaction.

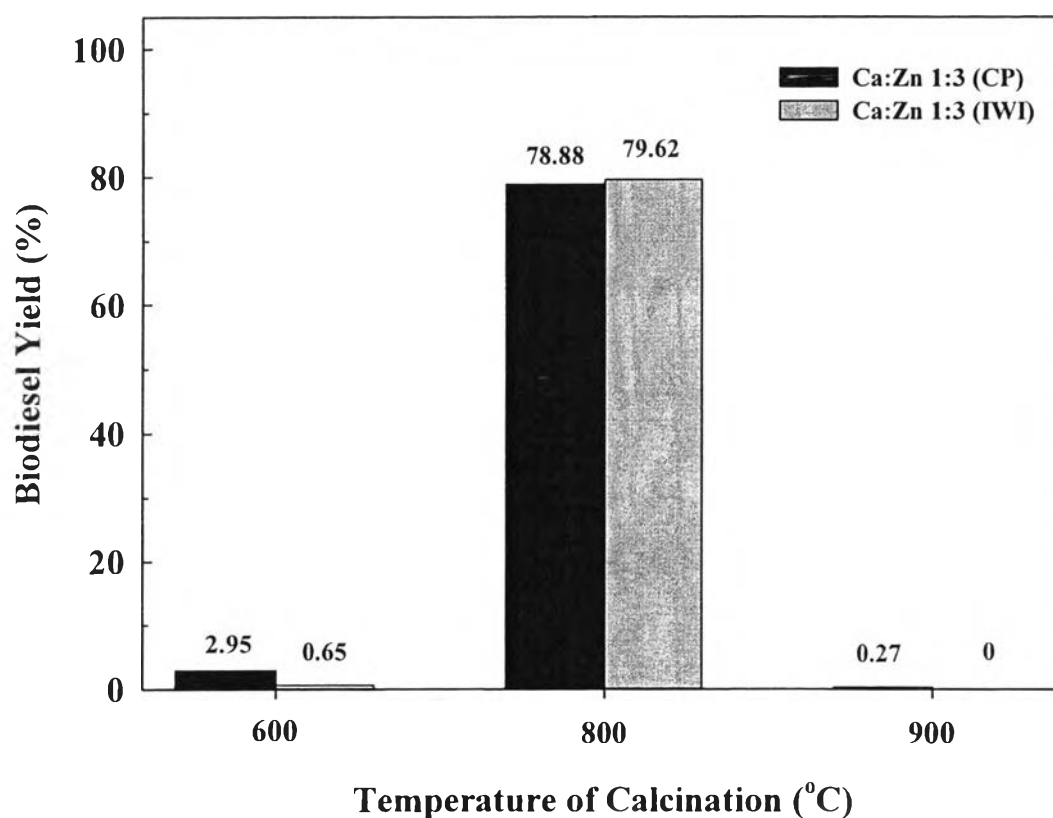


Figure 4.10 Effect of calcination temperature on biodiesel yield. Reaction conditions: 60 °C of reaction temperature, 8 h of reaction time, 1:3 atomic ratio of Ca:Zn, 15:1 molar ratio of methanol to oil, amount of catalyst 6 wt%, and 300 rpm of stirrer speed.

4.2.3 Effect of Ca:Zn Atomic Ratio

Many catalyst compositions (Ca:Zn atomic ratio) were considered at 1:5, 1:3, 1:1, and 3:1 respectively. Figure 4.11 revealed that the biodiesel yield was greatly effective on the variation of Ca:Zn atomic ratio. The highest biodiesel, approximately 78.88%, was observed in CP catalyst with Ca:Zn of 1:3, while the 80% biodiesel yield belonged to the IWI catalyst with the Ca:Zn range of 1:3–3:1. Focusing on the CP catalyst, the biodiesel yield was slightly decreased at high Ca concentrations. This was consistent with the appearance of CaO agglomeration, which has been reported in elsewhere (Ngamcharussrivichai *et al.*, 2008).

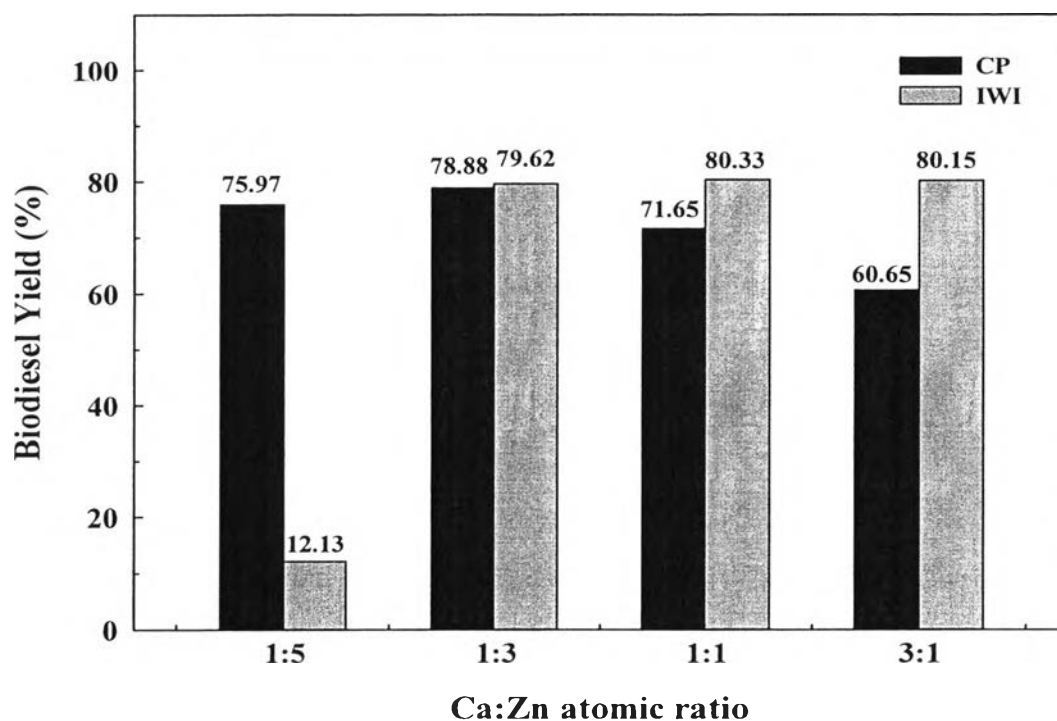


Figure 4.11 Effect of Ca:Zn atomic ratio on biodiesel yield. Reaction conditions: 60 °C of reaction temperature, 8 h of reaction time, 15:1 molar ratio of methanol to oil, amount of catalyst 6 wt%, and 300 rpm of stirrer speed.

4.2.4 Effect of Catalyst's Durability

Generally, the life time of the prepared catalyst is well known as one of the most important criterion for the commercialization. All of optimum conditions in the previous sections—8 h of reaction time, 1:3 atomic ratio of Ca:Zn, and calcination temperature of 800 °C—were constantly fixed to consider the catalyst's durability during the transesterification process at 60 °C of reaction temperature. The durability of the catalysts was applied for both IWI and CP techniques, as shown in Figure 4.12. For the first round operation, the IWI catalyst exhibited higher catalytic activity and achieved maximum biodiesel yield of 79.62 % when compared with that of CP catalyst (78.88 %). In the 2nd and 3rd running operations, the biodiesel yield dropped significantly for both samples. However, during the three cycles of catalyst's durability observation, the durability of the CaO–ZnO catalyst prepared by

IWI technique was much better than that of catalyst prepared by CP technique according to the higher amounts of CaO or Ca remaining on the surface of spent IWI catalyst (or less CaO leaching) after testing, which were confirmed by XRD and XRF results of the spent catalysts.

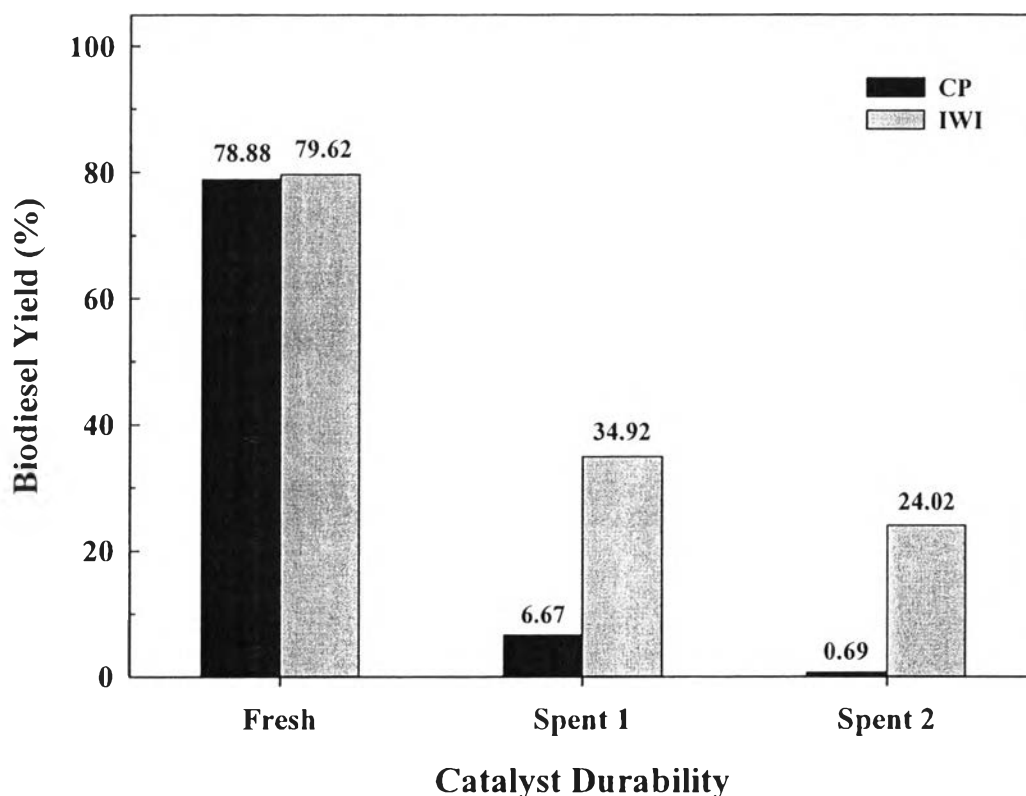


Figure 4.12 Durability of the CaO–ZnO catalysts on biodiesel yield. Reaction conditions: 60 °C of reaction temperature, 8 h of reaction time, 1:3 atomic ratio of Ca:Zn, 15:1 molar ratio of methanol to oil, amount of catalyst 6 wt%, and 300 rpm of stirrer speed.

The product distribution in the esteric phase over of the fresh CaO–ZnO catalysts was determined by HPLC analysis. The methyl ester yield, mono-, di-, and tri-glycerides of biodiesel were shown in Table 4.6 a) CP and b) IWI techniques. The highest methyl ester yield of 78.68 % and 79.33 % could be obtained from the catalysts prepared by CP and IWI, respectively, while the mono-, di-, and tri-glycerides contents turned to decrease due to the fact that the transesterification normally consists of a sequence of three consecutive and reversible reactions, which

have been mentioned in Chapter 2 already. In the first step, tri-glyceride is converted to diglyceride. After that, diglyceride is converted to monoglyceride, and monoglyceride is then converted to glycerol. For each step, one molecule of methyl ester is liberated, so the methyl ester increased with the decrease of the mono-, di-, and tri-glycerides since these three types of glyceride are converted to methyl ester.

Table 4.6 The methyl ester yield, mono-, di-, and tri-glycerides of biodiesel

Catalysts	Methyl ester (%)	Monoglyceride (%)	Diglyceride (%)	Triglyceride (%)
CaO–ZnO (1:3) (CP)	78.68	10.16	0	6.14
CaO–ZnO (1:3) (IWI)	79.33	5.05	0.69	12.33